RESEARCH ARTICLE

Check for updates

Carbon–carbon to boron–nitrogen isosterism enables switching toward fused 3D/2D magnetically aromatic systems

Zahra Noori [ID] *[a] and Jordi Poater [ID] *[a,b]

The realization of genuine 3D/2D aromatic systems through fusion of BN/CC isosteric azaborines with carborane clusters has been systematically examined using magnetic response analysis. Current density maps, bond current strengths, and DIAL surfaces demonstrate that magnetic descriptors provide the most sensitive criterion for multidimensional aromaticity. Although all isolated azaborines are aromatic, the magnitude and uniformity of their diatropic ring currents strongly depend on the number and relative positioning of BN units, with consecutive BN incorporation attenuating and polarizing the circulation. Fusion studies reveal that neither benzene nor mono-BN azaborine sustains integrated 3D/2D aromaticity due to a strong paratropic current localized at the fusion bond. In contrast, systems containing two consecutive BN/CC isosteres—particularly 1,4-diaza-2,3-diborine and 1,4-diaza-2-borine—exhibit a continuous diatropic ring current across the interface, consistent with effective magnetic communication between the planar ring and the boron cage. Electronic and energetic analyses support these findings but are less discriminating than magnetic criteria. Overall, this work establishes magnetic response properties as decisive tools for identifying viable 3D/2D aromatic systems and defines structural requirements for their design.

Introduction

BN/CC isosterism refers to the replacement of a carbon–carbon unit in an organic framework with an isoelectronic and isostructural boron–nitrogen pair, offering a powerful strategy to modulate electronic structure and chemical reactivity while largely retaining the original molecular geometry.[1] This approach has gained considerable attention because BN-containing analogues can closely resemble their all-carbon counterparts in shape and connectivity, yet display markedly different physicochemical properties arising from changes in polarity, hydrogen-bonding capability, and aromatic stabilization.[1–3] In monocyclic systems such as azaborines,[4] BN/CC isosterism systematically reduces aromatic stabilization relative to benzene, leading to distinct magnetic, energetic, and reactivity profiles. As a consequence, the energetic penalty associated with reactions that disrupt aromaticity is lowered,[1,5] enabling pericyclic processes that are otherwise unfavorable for purely carbon-based aromatics.[4,6,7]

An extreme manifestation of BN/CC isosterism is borazine (Fig. 1). Recent magnetic and energetic studies have shown that borazine—often termed "inorganic benzene"—possesses aromatic character,[8,9] albeit substantially weaker than that of benzene.[8,10–15] Magnetic response analyses by Pino-Rios et al. revealed the presence of a *hidden ring current* dominated by the π_3 orbital, which contributes in a manner analogous to the corresponding orbital in benzene.[16] In contrast, the degenerate π_1 and π_2 orbitals generate localized diatropic currents centered on the nitrogen atoms, effectively masking the global ring current. This weak aromaticity has also been corroborated experimentally by X-ray diffraction studies, which indicate island-like electronic delocalization within the B_3N_3 ring that primarily involves the nitrogen atoms.[15]

In parallel, icosahedral dicarbadodecaborane clusters $(C_2B_{10}H_{12})$, well known for their three-dimensional aromaticity,[17–20] have emerged as attractive building blocks for incorporation into extended molecular architectures due to their exceptional thermal stability and pronounced electron-withdrawing character when bonded to carbon atoms.[21,22] Nevertheless, the integration of carboranes into extended π-conjugated systems remains uncommon,[23–26] presenting an opportunity to expand chemical space beyond conventional two-dimensional polycyclic aromatic hydrocarbons.[27–30]

Despite this promise, we have recently demonstrated that, unlike many 2D/2D and 3D/3D aromatic fusions that preserve aromaticity, 3D/2D aromatic fusion is not viable.[23,24,31–33] This limitation arises from ineffective orbital overlap between the π

[a]Departament de Química Inorgànica i Orgànica & IQTCUB, Universitat de Barcelona, Martí i Franquès 1-11, 08028 Barcelona, Spain.
E-mail: jordi.poater@ub.edu
[b]ICREA, Passeig Lluís Companys 23, 08010 Barcelona, Spain
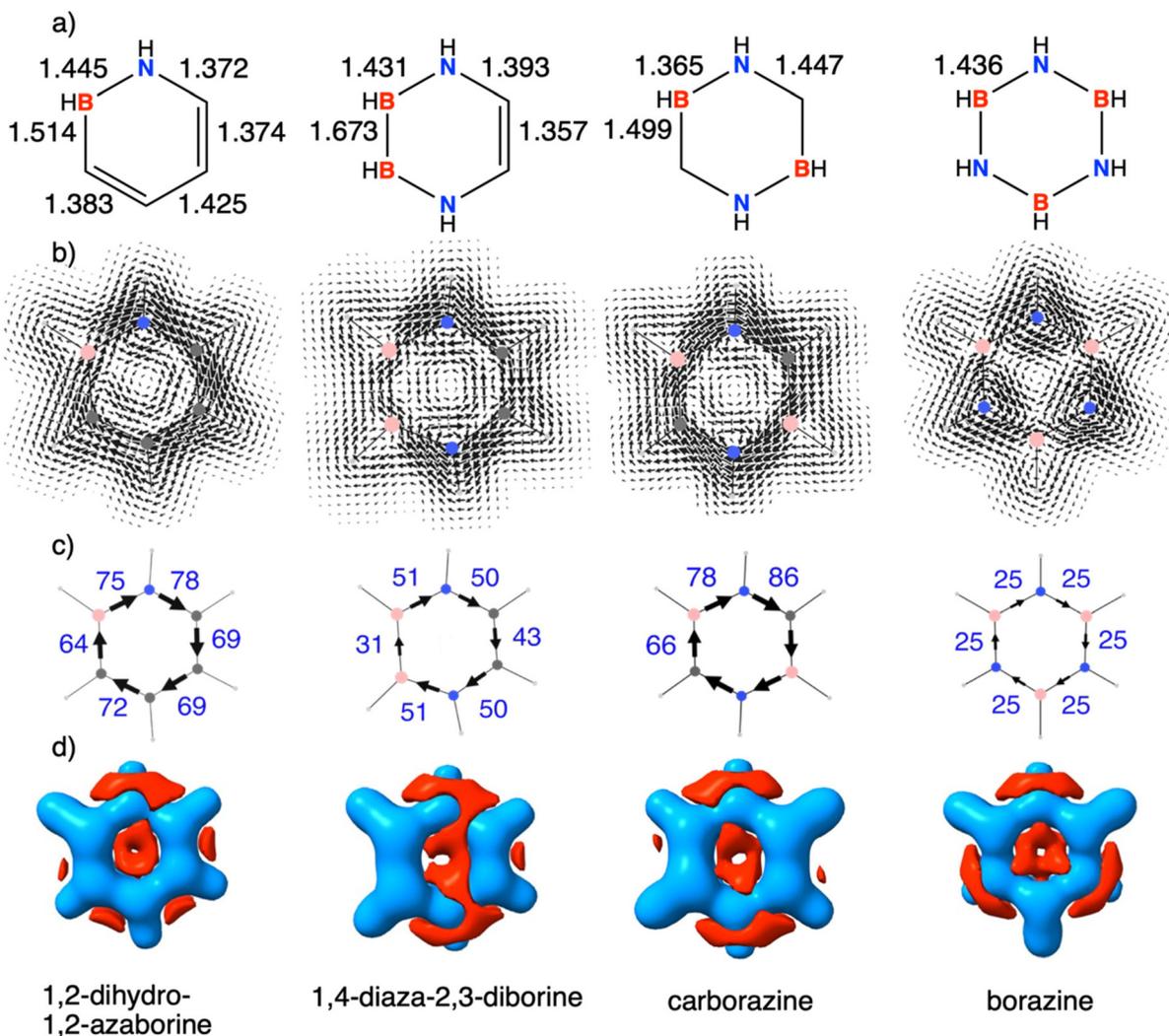
Fig. 1 Bond lengths of the ring (in Å) of 1,2-dihydro-1,2-azaborine, 1,4-diaza-2,3-diborine, carborazine, and borazine (a); current density maps for a perpendicular magnetic field computed on a plane located 1 a.u. below the molecular plane, with all (σ and π)-electron contributions (diatropic and paratropic circulations are clockwise and anticlockwise) (b); bond current strengths (c); and DIAL surfaces with diamagnetic regions shown in blue and paramagnetic regions shown in red (d). All systems are charged −1 except carborazine that is neutral.

molecular orbitals of the planar aromatic unit and the $(n + 1)$ molecular orbitals of the three-dimensional aromatic cage, which precludes efficient electronic delocalization across the fused system. Shortly thereafter, Kelemen and co-workers confirmed that this behavior also extends to *ortho*-carboranes fused with five-membered heterocycles.[34–36] In these systems, the position of the heteroatom within the *exo* ring dictates the bonding topology, resulting in restricted conjugation and the absence of aromatic stabilization. Moreover, the magnetic field generated by the 3D cluster perturbs the electronic structure of the fused *exo* ring, influencing calculated magnetic properties and potentially leading to erroneous assignments of aromatic character.[23,31,35]

To date, our studies have consistently shown a lack of double-bond character in the C–C, C–B, and B–B linkages connecting carboranes to planar aromatic units. However, this limitation may be overcome by directly coupling an electron-rich nitrogen atom to an electron-deficient boron atom at the fusion interface. In this context, BN/CC isosterism offers a promising strategy to enable effective 3D/2D conjugation and potentially restore aromatic communication between the two subunits. Motivated by this possibility, we herein investigate the aromaticity of a series of carboranes fused to azaborine motifs, aiming to assess whether BN incorporation can facilitate viable 3D/2D aromatic systems. In principle, achieving such effective 3D/2D aromatic communication should allow to expand the concept of aromaticity beyond planar systems, enabling cooperative delocalization between boron clusters and π-rings and providing new design principles for tuning electronic structure, stability, and magnetic response in hybrid molecular architectures.

Results and discussion

Our first azaborine reference system is 1,2-dihydro-1,2-azaborine, the simplest BN/CC isosteric analogue of benzene (Fig. 1). In comparison with benzene, which exhibits a homogeneous diatropic ring current density, the current distribution in 1,2-dihydro-1,2-azaborine is perturbed along the B–N bond, being weakened at the boron atom and enhanced at the nitrogen atom. Nevertheless, the pronounced diatropic bond current strengths observed along both the C–B and B–N bonds (64 and 75, respectively) clearly support its aromatic character. Upon introduction of two BN units, the diatropic ring current is further attenuated in 1,4-diaza-2,3-diborine,[37–39] with the effect being most pronounced at the B–B bond, in agreement with its reduced bond current strengths (31 and 51 for B–B and B–N bonds, respectively). In contrast, when the two BN units are spatially separated, as in carborazine (Fig. 1), the diatropic ring current remains comparable in magnitude to that of 1,2-dihydro-1,2-azaborine, supported by its stronger bond current strengths (66 and 78 for C–B and B–N, respectively). Finally, incorporation of three BN units, as in borazine, leads to the weakest diatropic ring current among the systems studied, showing the island-like main electronic delocalization on the N atoms,[15] a conclusion further supported by the corresponding bond current strengths (25 for B–N bond). But overall, although all four azaborine reference systems can be classified as aromatic, the degree of aromaticity is strongly dependent on both the number of BN units incorporated and their relative positioning within the six-membered ring.

Further insight on the above discussion can be obtained by means of the magnetically induced isotropically averaged Lorentz force density (DIAL) surfaces (Fig. 1 and Fig. S1). In the three azaborines studied, the enlarged paramagnetic regions around the B atoms in the surfaces indicate an enhancement of the paratropic components of the induced current and a weakening of the stable diatropic π circulation. In contrast, the opposite behavior is observed for the N atom.

Given that 1,4-diaza-2,3-diborine exhibits the weakest aromatic character among the azaborine systems examined, we next explored whether its aromaticity could be enhanced through electronic substitution. In particular, we evaluated the effect of introducing electron-donating groups at either the boron or nitrogen centers to strengthen aromatic delocalization. However, this strategy proved ineffective. Substitution at the boron atoms with strong electron donors such as NMe_2 or NH_2 further reduces aromaticity, as reflected by a weakened diatropic ring current density and smaller bond current strengths. For example, in system $BNMe_2$ (Fig. 2), the bond current strengths decrease to 16 and 18 for the B–B and B–N bonds, respectively. In contrast, alkyl substitution at the nitrogen atoms, including methyl or *tert*-butyl groups, has only a minor impact on the magnetic response; for instance, system NMe (Fig. 2) exhibits bond current strengths of 33 and 53 for the B–B and B–N bonds, respectively. This behavior can be rationalized in terms of a push–pull electronic effect between the nitrogen and boron atoms.[40] In such systems, electron-

donating substituents (*e.g.*, NMe_2 or NH_2) "push" electron density toward the electron-deficient boron centers within the conjugated heterocycle, which act as "pull" sites. Although this intramolecular charge-transfer interaction modifies the electronic distribution, it does not reinforce cyclic delocalization; instead, it perturbs the balance required for effective aromatic circulation. Consequently, electron-donating substitution at boron weakens the diatropic ring current—and thus the aromaticity—of 1,4-diaza-2,3-diborine, whereas substitution at nitrogen leaves it largely unaffected. This distinction is crucial and will be considered in the analysis of the fused systems with *nido*-carboranes discussed below.

As outlined above, the primary objective of the present work is to explore whether a viable 3D/2D aromatic system can be achieved through fusion of azaborine derivatives with *nido*-carborane $[C_2B_9H_{12}]^{-1}$. Previous studies have demonstrated that such 3D/2D aromatic conjugation cannot be realized when benzene is fused to a carborane cluster.[23,24,31–36,41,42] This limitation arises from the ineffective overlap between the π molecular orbitals (MOs) of the planar aromatic ring and the $(n + 1)$ MOs of the boron cage, which prevents efficient electronic delocalization between the two fragments. Magnetically, this is reflected in the very weak diatropic ring current along the five external bonds of benzene, which is disrupted by a strong paratropic ring current localized at the fusing C–C bond (Fig. 3). At difference there is a strong paratropic ring current inside the ring. Thus, for this *nido*-benzene, while the bond current strengths of the external bonds range only from 5 to 13, the paratropic current at the fusion bond reaches a markedly higher value of 79. When BN/CC isosterism is introduced by replacing benzene with 1,2-dihydro-1,2-azaborine, the formation of a 3D/2D aromatic system is still not achieved (Fig. 3). Despite the internal paratropic ring current has almost vanished, now we observe a stronger external non-uniform diatropic ring current. Thus, although the diatropic ring current within the azaborine ring increases significantly (bond current strengths of 58–70), the fusing C–B bond remains strongly paratropic (bond current strength of 55), thereby interrupting global delocalization.

Complementary insight is provided by the DIAL surfaces (Fig. 3), which reveal partial spatial merging of the diatropic currents of the 3D *nido*-carborane and the 2D azaborine units. Nevertheless, a pronounced paratropic contribution (shown in red) persists at the fusion bond, confirming its paratropic character and ultimately preventing the establishment of a fully integrated 3D/2D aromatic system.

Remarkably, a continuous diatropic ring current is observed when 1,4-diaza-2,3-diborine is fused to *nido*-carborane (Fig. 4). Upon incorporation of two BN/CC isosteric units, the fused B–B bond also exhibits a diatropic character (bond current strength of 55), indicating improved electronic communication across the interface. Nevertheless, the azaborine ring itself sustains only a modest diatropic ring current (bond current strengths of 13–16). Importantly, similar behavior is observed when the fusion occurs through a C–B bond. In the case of 1,4-diaza-2-borine fused to *nido*-carborane, the azaborine ring
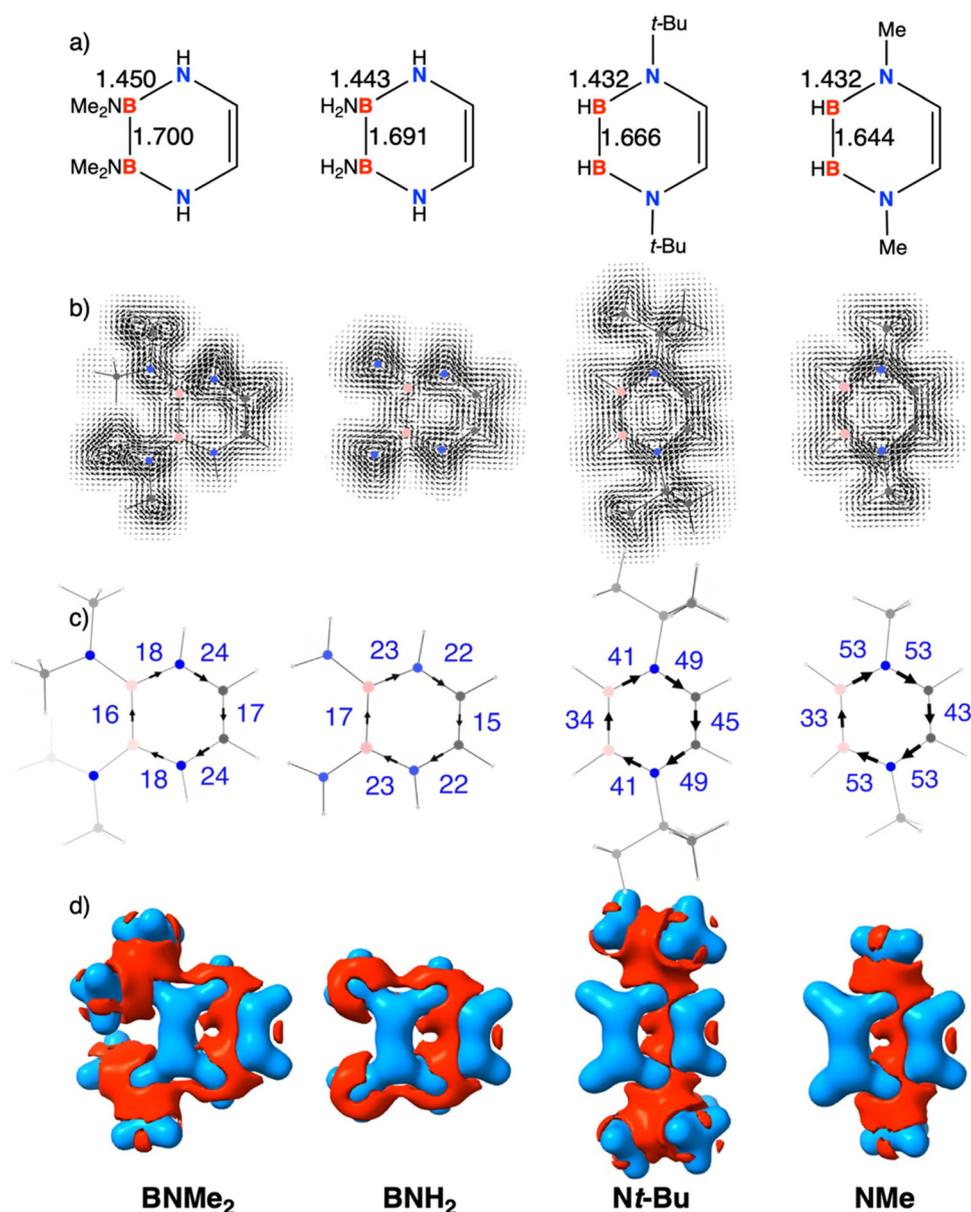
Fig. 2 Bond lengths of the ring (in Å) of substituted 4-diaza-2,3-diborine derivatives (a); current density maps for a perpendicular magnetic field computed on a plane located 1 a.u. below the molecular plane, with all (σ and π)-electron contributions (diatropic and paratropic circulations are clockwise and anticlockwise) (b); bond current strengths (c); and DIAL surfaces with diamagnetic regions shown in blue and paramagnetic regions shown in red (d). All systems are charged −1.

displays a somewhat stronger diatropic ring current (23–26), while the bond current strength at the fusion bond remains comparable (55).

In contrast, fusion of carborazine, despite also incorporating two BN/CC isosteric substitutions, does not yield a fully diatropic system (Fig. 4). Although the azaborine ring itself exhibits relatively strong diatropic currents (34–48), these are again disrupted by a paratropic contribution at the fusing C–B bond. These results demonstrate that the mere introduction of BN/CC isosterism is insufficient; rather, the relative positioning of the BN units within the azaborine framework is crucial

for achieving effective 3D/2D aromatic delocalization (see also Fig. S2).

Consistent with this magnetic analysis, the DIAL surfaces for the systems fused with 1,4-diaza-2,3-diborine or 1,4-diaza-2-borine clearly reveal a diatropic contribution along the fusion bond connecting the two aromatic units (Fig. 4). In contrast to the previously discussed systems, the paratropic regions (shown in red) are no longer localized at the fusion interface but instead are mainly associated with the lone pairs on the nitrogen atoms. However, this behavior is not observed for the *nido*-carborane–carborazine adduct, where the paratro-
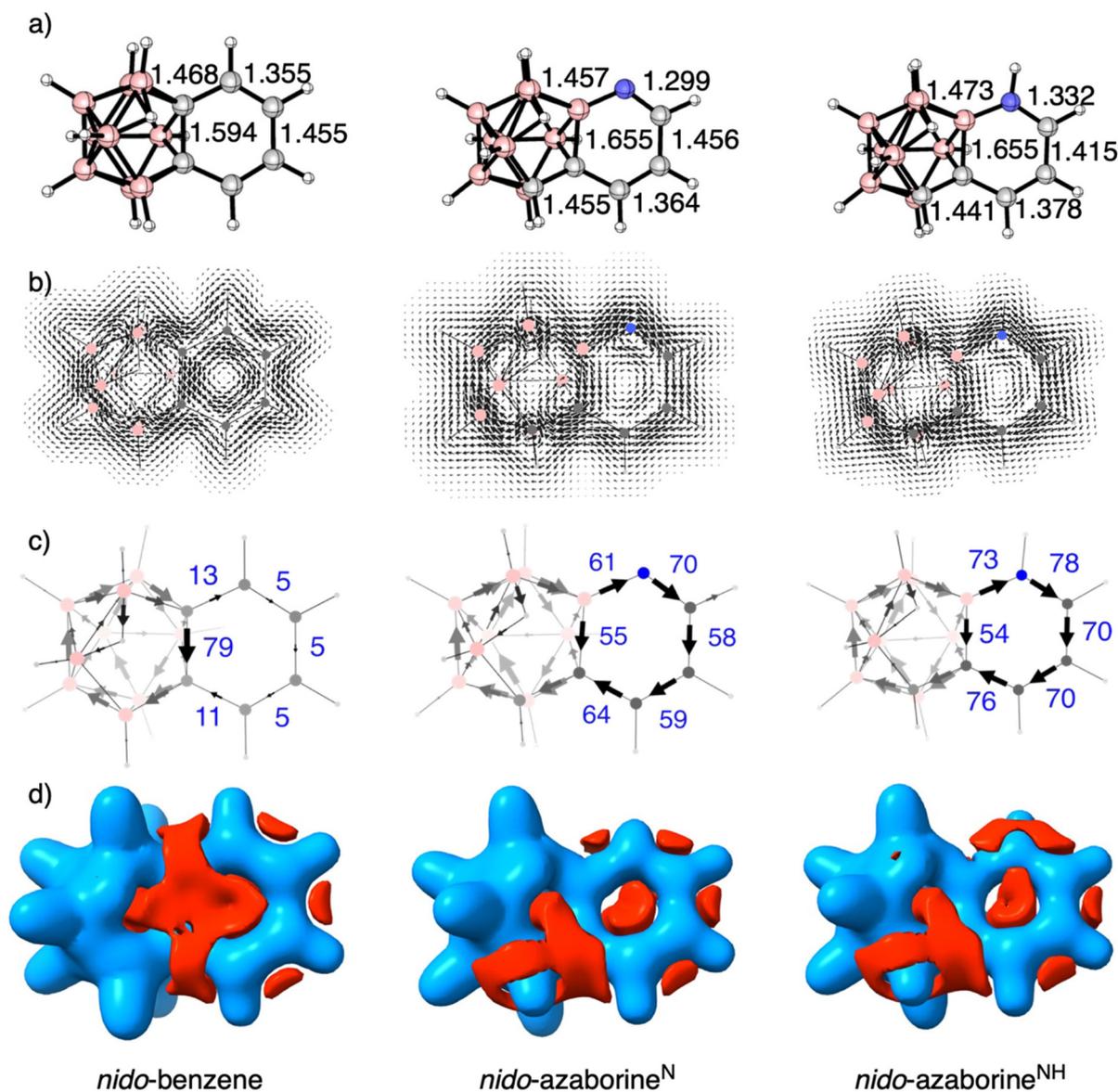
Fig. 3 Bond lengths of the ring (in Å) of fused *nido*-carborane to benzene and azaborine (a); current density maps for a perpendicular magnetic field computed on a plane located 1 a.u. below the molecular plane, with all (σ and π)-electron contributions (diatropic and paratropic circulations are clockwise and anticlockwise) (b); bond current strengths (c); and DIAL surfaces with diamagnetic regions shown in blue and paramagnetic regions shown in red (d). Systems *nido*-benzene and *nido*-azaborine[N] are charged −1, whereas *nido*-azaborine[NH] is neutral.

pic contribution remains concentrated at the fusing bond, further confirming the absence of a fully integrated 3D/2D aromatic system due to disruption at the interface.

For completeness, analogous fusions with *closo*-carborane were also investigated (Fig. 5). Notably, fusion of 1,4-diaza-2,3-diborine to *closo*-carborane also results in a fully diatropic ring current within the azaborine moiety, with even stronger bond current strengths than in the corresponding *nido* system (26–29 for the external bonds and 77 for the fused B–B bond).

Thus, the realization of a genuine 3D/2D aromatic system depends not only on the introduction of BN/CC isosterism but also critically on the relative positioning of the BN units within the azaborine framework. In addition, another key structural factor must be considered: the length of the fusion bond connecting the two aromatic fragments. In the case of benzene, the C–C bond involved in fusion elongates significantly from 1.400 Å in the isolated molecule to 1.594 Å upon fusion with *nido*-carborane (Fig. 3). Such pronounced lengthening effectively converts the bond into a single C–C bond, thereby disrupting π-conjugation and preventing electronic delocalization across the interface.

A similar situation is observed for the mono-BN isostere 1,2-dihydro-1,2-azaborine, where the fusion bond elongates from 1.514 Å in the isolated ring to 1.655 Å in the fused system
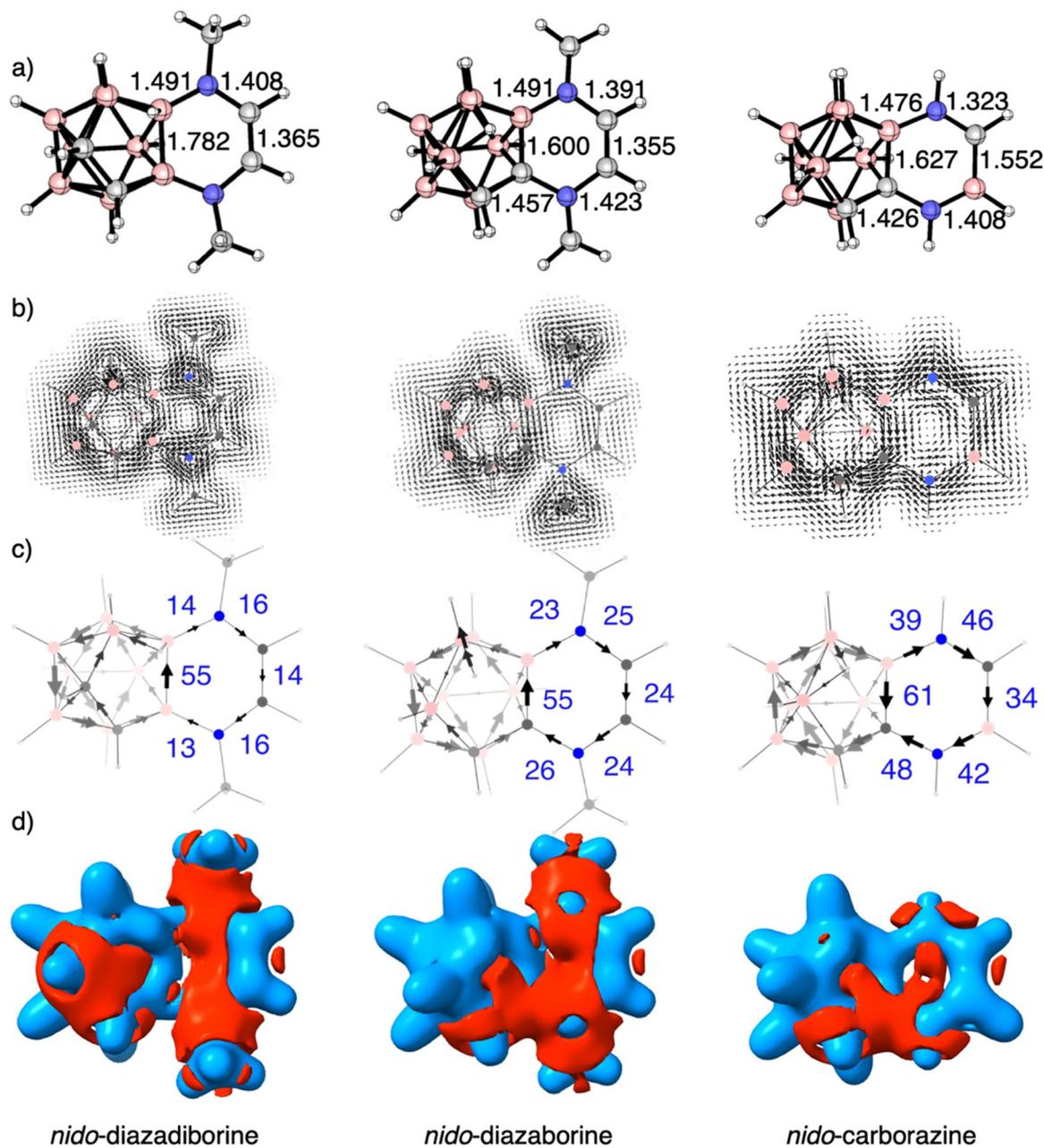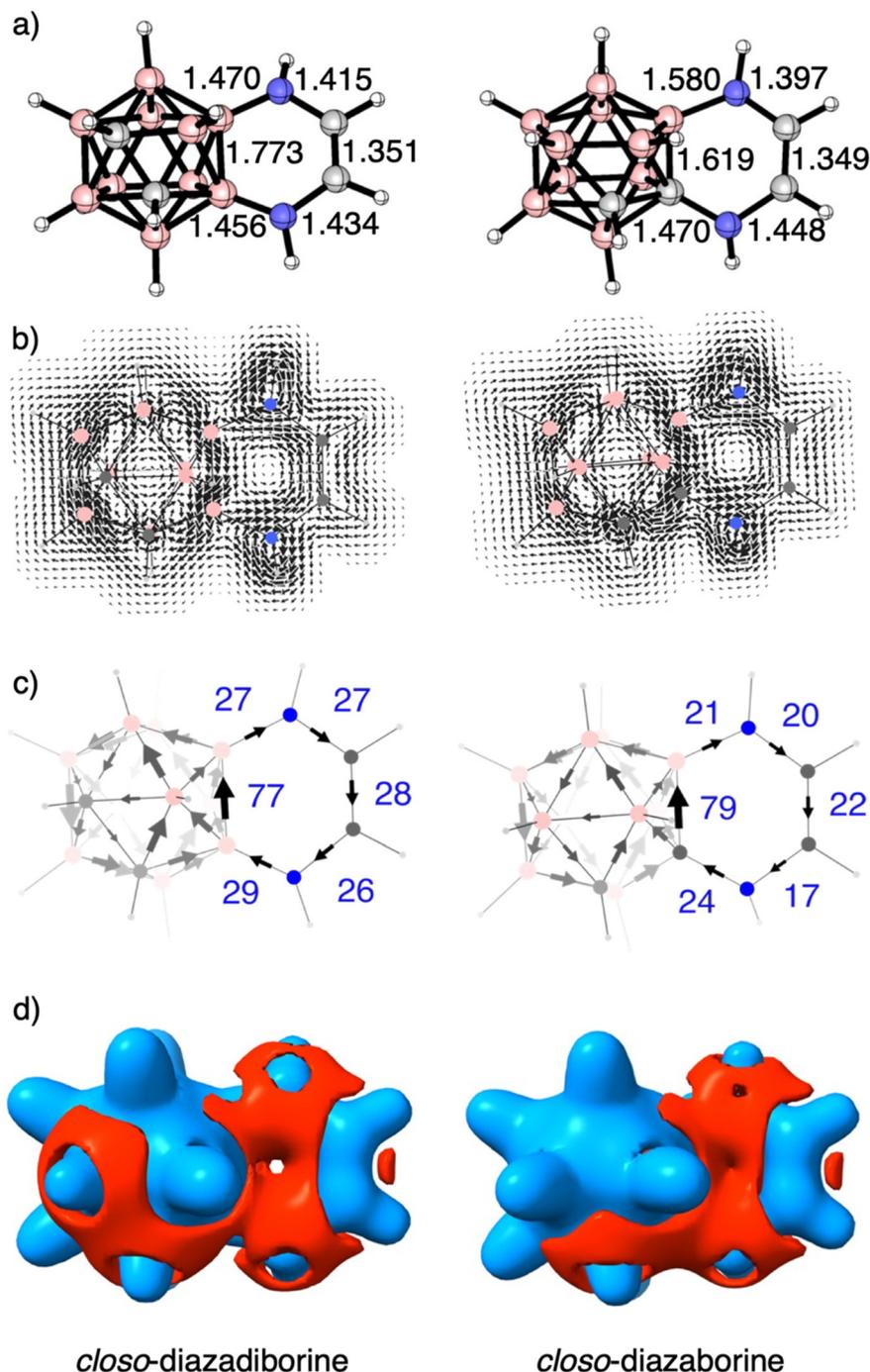
Fig. 4 Bond lengths of the ring (in Å) of fused *nido*-carborane $[C_2B_9H_{12}]^{-1}$ with 1,4-diaza-2,3-diborine, 1,4-diaza-2-borine, and carborazine (a); current density maps for a perpendicular magnetic field computed on a plane located 1 a.u. below the molecular plane, with all (σ and π)-electron contributions (diatropic and paratropic circulations are clockwise and anticlockwise) (b); bond current strengths (c); and DIAL surfaces with diamagnetic regions shown in blue and paramagnetic regions shown in red (d). Systems are charged −1.

(Fig. 3). This substantial increase in bond length again hampers effective 3D/2D electronic communication. In contrast, systems incorporating two consecutive BN/CC isosteres behave differently. For *nido*-1,4-diaza-2,3-diborine, the B–B fusion bond increases only moderately from 1.673 Å to 1.782 Å upon fusion (Fig. 4). Similarly, in *nido*-1,4-diaza-2-borine, the C–B bond length changes from 1.499 Å to 1.600 Å (Fig. 4). In both cases, the more limited bond elongation preserves a significant degree of π-delocalization within the azaborine ring

and facilitates effective electronic communication with the *nido*-carborane cluster. This structural feature ultimately enables the establishment of a continuous diatropic ring current in the 2D fragment upon fusion, consistent with the formation of a viable 3D/2D aromatic system.

At this point, it is worth referring to the previously claimed ineffective overlap between the π molecular orbitals (MOs) of benzene and the (n + 1) MOs of the boron cage.[31–33] At difference, diazodiborine ring, despite also presenting 6π electrons,

Fig. 5 Bond lengths of the ring (in Å) of fused *closo*-carborane with 1,4-diaza-2,3-diborine, and 1,4-diaza-2-borine (a); current density maps for a perpendicular magnetic field computed on a plane located 1 a.u. below the molecular plane, with all (σ and π)-electron contributions (diatropic and paratropic circulations are clockwise and anticlockwise) (b); bond current strengths (c); and DIAL surfaces with diamagnetic regions shown in blue and paramagnetic regions shown in red (d). Systems are charged −1.

the electronegativity difference between B and N atoms causes a strong orbital polarization (Fig. S3). Its electronic delocalization is present, but not uniform any longer, together with a different energetic ordering compared to fully symmetric benzene. Such distortion of the heterocyclic ring translates into a stronger overlap between the π fragment molecular orbi-

tals of this ring and the *nido*-carborane (Fig. S4 and Table S1). This latter further supports the diatropic ring current above observed for this heterocycle in *nido*-diazadiborine compared to *nido*-benzene. This data is obtained from an energy decomposition analysis performed on both fused *nido*-diazadiborine compared to *nido*-benzene systems (Table S1), with the

former showing a weaker interaction between 3D and 2D units (-209.2 and -245.4 kcal mol^{-1}, respectively). Furthermore, in 1,4-diaza-2,3-diborine when fused to *nido*-carborane, negative hyperconjugation arises from donation of electron density from polarized π orbitals (mainly N-centered) into antibonding orbitals of the electron-deficient boron atoms and the *nido*-carborane cage, thereby enhancing cage–ring coupling and contributing to the observed aromatic response.[43,44]

Last but not least, the discussion above supporting the formation of a fully integrated 3D/2D aromatic system through BN/CC isosterism has been based primarily on magnetic criteria of aromaticity. However, aromaticity is a multidimensional concept and, since it is not a directly observable property, it is generally characterized by two essential features: electron delocalization and energetic stabilization.[45–50] The absence of either of these components should preclude the assignment of aromatic character. Consequently, the previous conclusions based solely on magnetic descriptors must be complemented with an analysis of electronic delocalization. To this end, we computed delocalization indices (DIs) within the Atoms-in-Molecules (AIM) framework,[51] which provide a quantitative measure of electron sharing between pairs of atoms. In the case of benzene, the DI(C–C) value decreases markedly from 1.389 a.u. in the isolated ring to 0.984 a.u. upon fusion with *nido*-carborane (Fig. 6). This substantial reduction clearly indicates loss of electron delocalization at the fusion bond. Furthermore, the DIs within the fused benzene ring reveal localization into distinct single and double bonds, in sharp contrast to the uniform delocalization expected for an aromatic system. In contrast, for 1,4-diaza-2,3-diborine, the DI values for the B–B and B–N bonds are 0.812 and 0.708 a.u., respectively, in the isolated molecule. Upon fusion, these values decrease to 0.498 and 0.572 a.u., respectively—changes that are significantly smaller than those observed for benzene. Moreover, the DI associated with the formally localized C–C bond increases only slightly, from 1.558 to 1.601 a.u., upon fusion. This comparatively modest variation in electron delocalization supports the distinct behavior of 1,4-diaza-2,3-diborine and is consistent with its ability to sustain a fully integrated 3D/2D aromatic system.

Finally, for completeness, isomerization stabilization energies (ISEs) were computed as an energetic criterion of aromaticity. In their isolated forms, both 1,2-dihydro-1,2-azaborine and 1,4-diaza-2,3-diborine exhibit smaller ISE values than benzene, consistent with their reduced aromatic character (Fig. 7). For example, the ISE decreases from -32.5 kcal mol^{-1} for benzene to -16.7 kcal mol^{-1} for 1,4-diaza-2,3-diborine, reflecting the weaker energetic stabilization associated with BN incorporation. Upon fusion with *nido*-carborane, all systems retain negative ISE values, indicating that they remain energetically aromatic (Fig. 7), and the trends are kept, from -51.7 to -11.8 kcal mol^{-1} for benzene and 1,4-diaza-2,3-diborine fused to *nido*-carborane, respectively. However, we must be careful with the computed ISE values for such fused systems as, upon fusion, the *nido*-carborane fragment becomes the dominant electronic perturbation in both systems. Thus, the
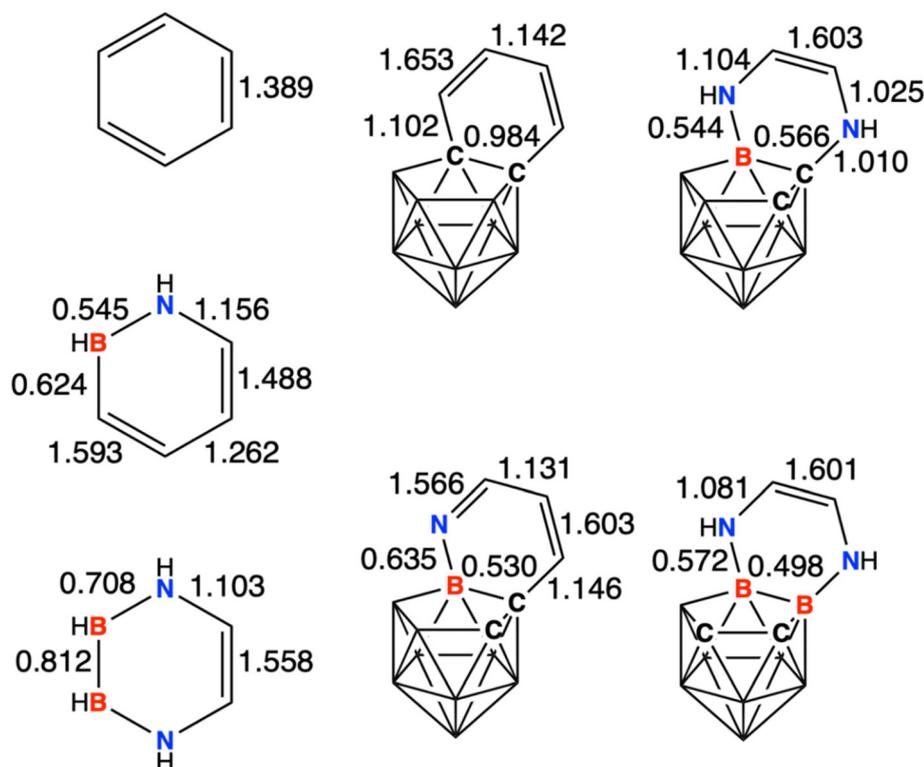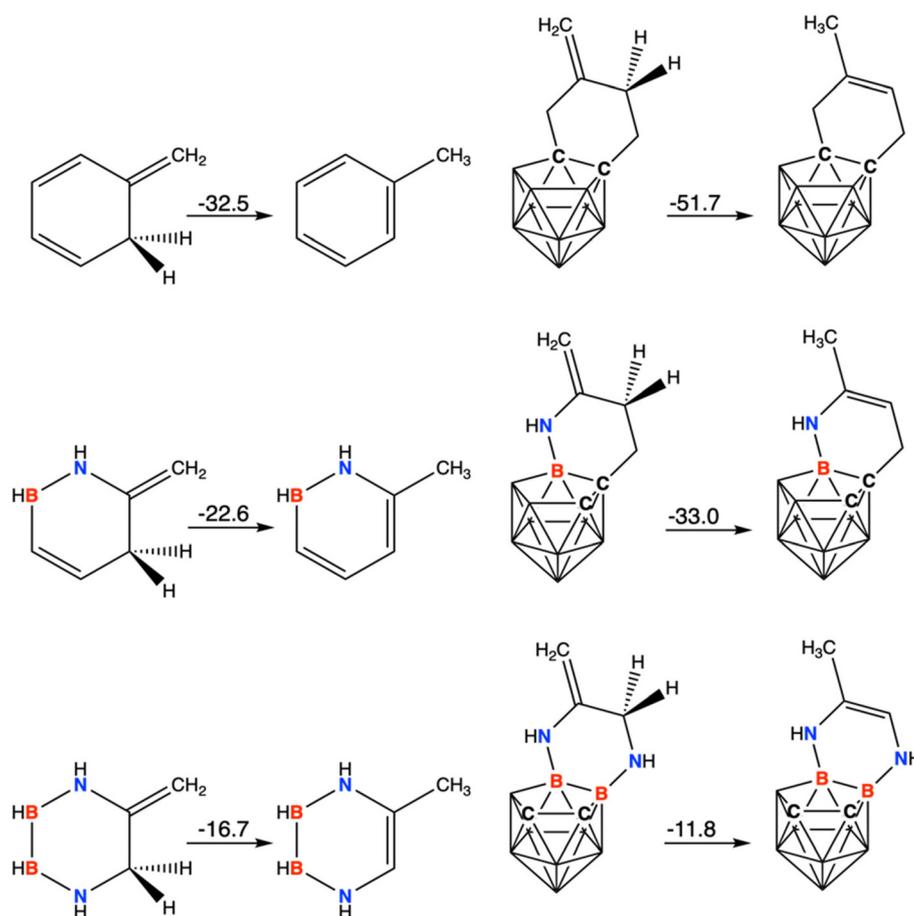

Fig. 6 Delocalization indices (in a.u.) of the azoborine rings under analysis, together with benzene for comparison.

Fig. 7 Isomerization stabilization energies (in kcal mol^{-1}) of methylated benzene (top), 1,2-dihydro-1,2-azaborine (middle), and 1,4-diaza-2,3-dibor-ine (bottom) alone (left) and when fused to *nido*-carborane (right). All fused systems are charged −1. CH$_2$ isomer for *nido*-benzene has a triplet state 4.7 kcal mol^{-1} lower in energy.

measured stabilization reflects not only the intrinsic aromaticity of benzene or diazadiborine, but also a comparable degree of cage–ring conjugation, polarization, and fusion-induced structural reorganization. Furthermore, we must also be cautious with these ISE values because the CH$_2$ isomers of both fused benzene and 1,2-dihydro-1,2-azaborine present an important biradical character, with the risk of describing the instability of the biradical rather than their aromaticity.

Thus, in the set of systems under analysis, although both the delocalization indices and the ISE values support the persistence of aromatic stabilization in the azaborine rings fused to *nido*-carborane, these energetic and electronic descriptors alone do not clearly distinguish which systems achieve genuine 3D/2D aromatic communication. In contrast, the magnetic descriptors—namely, ring current densities and bond current strengths—provide a more sensitive criterion for identifying the systems that sustain effective 3D/2D aromatic delocalization. For completeness, NICS have also been computed to further support the aromaticity of the carborane cages, either alone or fused to 2D aromatic systems (Table S2).[23–26,52–55] Nonetheless, NICS drive to misleading

conclusions for these fused 2D aromatic rings, as the magnetic field generated by the *nido*-carborane may influence the magnetic properties and conjugation of the fused 2D ring.[32,33] Also, and in agreement with previous works, MCI gives values very close to zero when dealing with electron-deficient rings involving boron.

Conclusions

The present study demonstrates that magnetic criteria seem to provide the most decisive evidence for assessing aromaticity and, in particular, for identifying genuine 3D/2D aromatic communication in azaborine–carborane fused systems. Current density maps, bond current strengths, and DIAL surfaces consistently reveal how BN/CC isosterism and structural arrangement govern the continuity—or disruption—of diatropic ring currents.

The isolated azaborine reference systems exhibit diatropic circulation and can therefore be classified as aromatic. However, both the magnitude and uniformity of the ring current strongly depend on the number and relative position-

ing of BN units. Incorporation of consecutive BN fragments attenuates the global diatropic current, whereas spatial separation of BN units preserves a stronger and more uniform circulation. This reduction in aromaticity is reflected in increasingly perturbed diatropic ring currents and is further quantified by lower bond current strengths.

Fusion with carborane clusters provides the most striking insights. In agreement with previous studies, fusion of benzene or mono-BN azaborine to *nido*-carborane fails to generate a unified aromatic system. The magnetic response is dominated by a strong paratropic current at the fusion bond, which interrupts global diatropic circulation despite residual aromaticity within each fragment. Bond current strengths and DIAL surfaces unequivocally show that this paratropic contribution prevents effective 3D/2D delocalization. In contrast, when two consecutive BN/CC isosteres are incorporated—specifically in 1,4-diaza-2,3-diborine and 1,4-diaza-2-borine—a continuous diatropic ring current across the fusion interface is achieved. The fusion bond itself becomes diatropic. Importantly, the success of these systems correlates with limited elongation of the fusion bond, preserving the magnetic continuity necessary for effective 3D/2D aromatic communication. By contrast, carborazine fusion—despite BN incorporation—retains a paratropic fusion bond, underscoring that relative BN positioning, rather than mere BN substitution, is the determining factor.

Electronic (delocalization indices) and energetic (ISE) analyses support the magnetic findings but play a complementary role. While these descriptors confirm the persistence of aromatic stabilization and reveal better preservation of electron sharing in the successful diaza-diborine systems compared to benzene, they do not as clearly discriminate between systems that achieve true 3D/2D aromatic integration and those that do not.

Overall, this work establishes that achieving a viable 3D/2D aromatic system requires not only BN/CC isosterism but precise control over BN positioning and structural adaptation at the fusion interface, providing clear magnetic-based design principles for future heteroaromatic architectures.

Theoretical methods

All calculations were performed with the AMS software[56–59] at the ZORA-BLYP-D3(BJ)/TZ2P level of theory. The geometry optimizations were carried out without symmetry constraints and analytical hessians were computed to characterize the optimized structures as minima (zero imaginary frequencies). Aromaticity was first evaluated by means of the nucleus-independent chemical shift (NICS),[46,54,60,61] proposed by Schleyer and co-workers as a magnetic descriptor of aromaticity. NICS is defined as the negative value of the absolute shielding computed at a ring center or at some other point of the system. Rings with large negative NICS values are considered aromatic. NICS values were computed using the gauge-including atomic orbital method (GIAO).[62] Delocalization indices (DIs) and multicenter indices (MCI)[25,26,63–65] were computed with the ESI-3D program using AIM partition of space.[66,67]

Current density maps have been computed by means of the SYSMOIC package[68–70] with the B3LYP hybrid density functional and the 6-311++G(d,p) basis set, for a perpendicular magnetic field over a plane 1 a.u. below the molecular plane.[71–73] Red/blue arrows when the component parallel/antiparallel to the magnetic field **B** is greater than 30% of the vector modulus. Diatropic/paratropic circulations are clockwise/anticlockwise.[10] With respect to the bond current strengths, values aside each arrow represent the percentage relationship with respect to a reference current strength of 12 nA T^{-1}. Noticeably, the current density maps distinguish the roles of σ and π electrons in aromatic systems. σ-electrons form the local bonding framework and create localized vortices around individual bonds, including paratropic currents at ring centers. In contrast, delocalized π-electrons generate a global ring current under an external magnetic field, leading to shielding inside the ring and deshielding outside it. At about 1 a.u. above or below the ring plane, the total current density is dominated by the more mobile π-electrons, whose global circulation masks the weaker, localized σ contributions. The non-uniform diatropic and paratropic currents suggest weaker aromaticity compared to benzene, which serves as a reference. While current density maps provide qualitative insight, bond current strength calculations were performed to quantitatively assess electron delocalization, with values expressed as percentages relative to benzene.[10,12,68–70,74]

Finally, we have also included the magnetically induced isotropically averaged Lorentz force density (DIAL) which is a real-space descriptor derived from the Lorentz force formalism and adapted to the quantum-mechanical description of electrons in molecules.[10,74] Under an external magnetic field, the electronic response is expressed through the magnetically induced current density $J(r)$, from which the Lorentz force density can be obtained. To remove dependence on the field orientation, the current density tensor is used to perform isotropic averaging, yielding the isotropically averaged Lorentz force density (IALFD). The divergence of the IALFD (DIAL) provides chemically meaningful insight by identifying regions where induced currents are locally reinforced or depleted. Diamagnetic regions are typically associated with stable circulating currents and aromatic stabilization, whereas paramagnetic regions indicate local perturbations. This orientation- and origin-independent approach is particularly well suited for analyzing non-planar and structurally complex systems. In these surfaces, diamagnetic regions (diatropic contributions) are shown in blue, while paramagnetic regions (paratropic contributions) are shown in red. The surfaces are displayed at two isovalues: −0.001 a.u. (blue) and +0.006 a.u. (red), considering all-electron contributions.

Author contributions

Zahra Noori performed the quantum chemical computations, analyzed the results, and wrote a first draft. Jordi Poater planned the project and wrote the manuscript.

Conflicts of interest

There are no conflicts to declare.

Data availability

Supplementary information (SI): Cartesian coordinates of all systems under analysis, complementary figures of the current density maps, and NICS values. See DOI: **https://doi.org/10.1039/d6qo00257a**.

Acknowledgements

References

1 M. J. D. Bosdet and W. E. Piers, B-N as a C-C substitute in aromatic systems, *Can. J. Chem.*, 2009, **87**, 8–29.

2 L. Kong and C. Cui, Perspective on Organoboron Chemistry, *Synlett*, 2021, 1316–1322.

3 B. Su and R. Kinjo, Construction of Boron-Containing Aromatic Heterocycles, *Synthesis*, 2017, 2985–3034.

4 P. G. Campbell, A. J. V. Marwitz and S.-Y. Liu, Recent Advances in Azaborine Chemistry, *Angew. Chem., Int. Ed.*, 2012, **51**, 6074–6092.

5 H. C. Söyleyici, S. Uyanık, R. Sevinçek, E. Fırıncı, B. Bursalı, O. Burgaz, M. Aygün and Y. Şahin, Synthesis and structures of monocyclic 1,4-diaza-2,3-diborine species, *Inorg. Chem. Commun.*, 2015, **61**, 214–216.

6 H. M. Robichaud, J. S. A. Ishibashi, T. Ozaki, W. Lamine, K. Miqueu and S.-Y. Liu, The aromatic Claisen rearrangement of a 1,2-azaborine, *Org. Biomol. Chem.*, 2023, **21**, 3778–3783.

7 Z. X. Giustra and S.-Y. Liu, The State of the Art in Azaborine Chemistry: New Synthetic Methods and Applications, *J. Am. Chem. Soc.*, 2018, **140**, 1184–1194.

8 B. Kiran, A. K. Phukan and E. D. Jemmis, Is Borazine Aromatic? Unusual Parallel Behavior between Hydrocarbons and Corresponding B−N Analogues, *Inorg. Chem.*, 2001, **40**, 3615–3618.

9 E. D. Jemmis and B. Kiran, Aromaticity in $X_3Y_3H_6$ (X = B, Al, Ga; Y = N, P, As), $X_3Z_3H_3$ (Z = O, S, Se), and Phosphazenes. Theoretical Study of the Structures, Energetics, and Magnetic Properties, *Inorg. Chem.*, 1998, **37**, 2110–2116.

10 G. Monaco and R. Zanasi, The molecular electronic structure revealed by the magnetically induced Lorentz force density, *J. Chem. Phys.*, 2020, **153**, 104114.

11 Y. Wu, X. Yan, Z. Liu, T. Lu, M. Zhao, J. Xu and J. Wang, Aromaticity in Isoelectronic Analogues of Benzene, Carborazine and Borazine, from Electronic Structure and Magnetic Property, *Chem. – Eur. J.*, 2024, **30**, e202403369.

12 M. Orza, F. F. Summa, R. Zanasi and G. Monaco, A Study of Differential Topology on the Magnetically Induced Isotropically Averaged Lorentz Force Density of a Few Simple Molecules, *Molecules*, 2024, **29**, 4502.

13 R. Islas, D. Arias-Olivares, A. Becerra-Buitrago, L. C. García-Sánchez, L. N. Méndez-Ayón and B. Zuniga-Gutierrez, Metallaborazines: To Be or Not To Be Delocalized, *ACS Omega*, 2021, **6**, 19629–19641.

14 P. Preethalayam, N. Proos Vedin, S. Radenković and H. Ottosson, Azaboracyclooctatetraenes reveal that the different aspects of triplet state Baird-aromaticity are nothing but different, *J. Phys. Org. Chem.*, 2023, **36**, e4455.

15 M. d. R. Merino-García, L. A. Soriano-Agueda, J. d. D. Guzmán-Hernández, D. Martínez-Otero, B. Landeros Rivera, F. Cortés-Guzmán, J. E. Barquera-Lozada and V. Jancik, Benzene and Borazine, so Different, yet so Similar: Insight from Experimental Charge Density Analysis, *Inorg. Chem.*, 2022, **61**, 6785–6798.

16 R. Báez-Grez and R. Pino-Rios, The hidden aromaticity in borazine, *RSC Adv.*, 2022, **12**, 7906–7910.

17 R. Chaliha, D. S. Perumalla, K. Yadav, D. L. V. K. Prasad and E. D. Jemmis, An Extended Rudolph Diagram: B_3H_5 and $B_3H_6^+$ Relate 3D-, 2D-, 1D-, and 0D-Boron Allotropes, *Inorg. Chem.*, 2024, **63**, 10954–10966.

18 A. Muñoz-Castro, Interplay Between Planar and Spherical Aromaticity: Shielding Cone Behavior in Dual Planar-Planar, Planar-Spherical and Spherical-Spherical Aromatics, *ChemPhysChem*, 2020, **21**, 1384–1387.

19 O. Shameema and E. D. Jemmis, Relative Stability of *closo-closo*, *closo-nido*, and *nido-nido* Macropolyhedral Boranes: The Role of Orbital Compatibility, *Chem. – Asian J.*, 2009, **4**, 1346–1353.

20 K. Vidya and E. D. Jemmis, Relative stabilities of condensed face sharing mono- and di-carboranes: $CB_{20}H_{18}$ and $C_2B_{19}H_{18}^+$, *J. Organomet. Chem.*, 2015, **798**, 91–98.

21 M. O. Akram, J. R. Tidwell, J. L. Dutton, D. J. D. Wilson, A. Molino and C. D. Martin, Accessing Boron-Doped Pentaphene Analogues from 12-Boradibenzofluorene, *Inorg. Chem.*, 2022, **61**, 9595–9604.

22 M. O. Akram, J. R. Tidwell, J. L. Dutton and C. D. Martin, Bis(1-Methyl-ortho-Carboranyl)Borane, *Angew. Chem., Int. Ed.*, 2023, **62**, e202307040.

23 F. Sun, S. Tan, H.-J. Cao, C.-s. Lu, D. Tu, J. Poater, M. Solà and H. Yan, Facile Construction of New Hybrid Conjugation via Boron Cage Extension, *J. Am. Chem. Soc.*, 2023, **145**, 3577–3587.

24 Z. Sun, J. Zong, H. Ren, C. Lu, D. Tu, J. Poater, M. Solà, Z. Shi and H. Yan, Couple-close construction of non-classical boron cluster-phosphonium conjugates, *Nat. Commun.*, 2024, **15**, 7934.

25 D. Tu, J. Li, F. Sun, H. Yan, J. Poater and M. Solà, Cage–···Cage– Interaction: Boron Cluster-Based Noncovalent Bond and Its Applications in Solid-State Materials, *JACS Au*, 2021, **1**, 2047–2057.

26 D. Tu, H. Yan, J. Poater and M. Solà, The nido-Cage···π Bond: A Non-covalent Interaction between Boron Clusters and Aromatic Rings and Its Applications, *Angew. Chem., Int. Ed.*, 2020, **59**, 9018–9025.

27 Y. Li, M. Tamizmani, M. O. Akram and C. D. Martin, Carborane–arene fused boracyclic analogues of polycyclic aromatic hydrocarbons accessed by intramolecular borylation, *Chem. Sci.*, 2024, **15**, 7568–7575.

28 Y. Nie, J. Miao, H. Wadepohl, H. Pritzkow, T. Oeser and W. Siebert, Syntheses and Characterization of o-Carboranes Containing Fused exo-Polyhedral Di- and Triboraheterocycles, *Z. Anorg. Allg. Chem.*, 2013, **639**, 1188–1193.

29 J. Krebs, A. Häfner, S. Fuchs, X. Guo, F. Rauch, A. Eichhorn, I. Krummenacher, A. Friedrich, L. Ji, M. Finze, Z. Lin, H. Braunschweig and T. B. Marder, Backbone-controlled LUMO energy induces intramolecular C–H activation in ortho-bis-9-borafluorene-substituted phenyl and o-carboranyl compounds leading to novel 9,10-diboraanthracene derivatives, *Chem. Sci.*, 2022, **13**, 14165–14178.

30 M. Zhong, J. Zhang, Z. Lu and Z. Xie, Diboration of alkenes and alkynes with a carborane-fused four-membered boracycle bearing an electron-precise B–B bond, *Dalton Trans.*, 2021, **50**, 17150–17155.

31 J. Poater, C. Viñas, M. Solà and F. Teixidor, 3D and 2D aromatic units behave like oil and water in the case of benzocarborane derivatives, *Nat. Commun.*, 2022, **13**, 3844.

32 Z. Noori, M. Solà, C. Viñas, F. Teixidor and J. Poater, Unraveling aromaticity: the dual worlds of pyrazole, pyrazoline, and 3D carborane, *Beilstein J. Org. Chem.*, 2025, **21**, 412–420.

33 Z. Noori and J. Poater, Aromaticity switch of borabenzene: from aromatic when free or weakly aromatic when fused to 2D PAHs to non-aromatic when fused to 3D carboranes, *Org. Chem. Front.*, 2025, **12**, 4321–4331.

34 D. Buzsaki, M. B. Kovacs, E. Humpfner, Z. Harcsa-Pinter and Z. Kelemen, Conjugation between 3D and 2D aromaticity: does it really exist? The case of carborane-fused heterocycles, *Chem. Sci.*, 2022, **13**, 11388–11393.

35 Z. Kelemen, D. Buzsáki, D. Gál, Z. Harcsa-Pintér and L. Kalabay, The possible aromatic conjugation via the different edges of (car)borane clusters – Can the relationship between 3D and 2D aromatic systems be reconciled?, *Chem. – Eur. J.*, 2024, **30**, e202402970.

36 D. Gál, L. Szántai, D. Buzsáki and Z. Kelemen, Unveiling the True Identity of Carborane-Fused Phosphorus Heterocycles, *Org. Lett.*, 2025, **27**, 5637–5641.

37 X. Liu, Y. Zhang, B. Li, L. N. Zakharov, M. Vasiliu, D. A. Dixon and S.-Y. Liu, A Modular Synthetic Approach to Monocyclic 1,4-Azaborines, *Angew. Chem., Int. Ed.*, 2016, **55**, 8333–8337.

38 T. Thiess, M. Ernst, T. Kupfer and H. Braunschweig, Facile Access to Substituted 1,4-Diaza-2,3-Diborinines, *Chem. – Eur. J.*, 2020, **26**, 2967–2972.

39 M. Arrowsmith, H. Braunschweig, K. Radacki, T. Thiess and A. Turkin, Facile Access to Unprecedented Electron-Precise Monohydrodiboranes(4), cis-1,2-Dihydrodiboranes (4), and a 1,1-Dihydrodiborane(5), *Chem. – Eur. J.*, 2017, **23**, 2179–2184.

40 A. J. Ruddy, D. M. C. Ould, P. D. Newman and R. L. Melen, Push and pull: the potential role of boron in N2 activation, *Dalton Trans.*, 2018, **47**, 10377–10381.

41 A. B. Buades, Z. Kelemen, V. S. Arderiu, A. Zaulet, C. Viñas and F. Teixidor, A fast and simple B-C bond formation in metallacarboranes avoiding halometallacarboranes and transition metal catalysts, *Dalton Trans.*, 2020, **49**, 3525–3531.

42 I. Guerrero, Z. Kelemen, C. Viñas, I. Romero and F. Teixidor, Metallacarboranes as Photoredox Catalysts in Water, *Chem. – Eur. J.*, 2020, **26**, 5027–5036.

43 D. Buzsáki, D. Gál, B. Szathmári, T. Holczbauer, A. Udvardy, J. K. Szilágyiné, D. Kargin, C. Bruhn, R. Pietschnig and Z. Kelemen, The "chemical tug-of-war" in carborane clusters: distinct tuning on different sides of the cluster, *Inorg. Chem. Front.*, 2025, **12**, 1822–1830.

44 Y. Gao, B. Szathmári, D. Buzsáki and Z. Kelemen, Reassessing the Possibility of π–σ–π Full Electron Delocalization Through 3D Aromatic Carboranes, *Chem. – Eur. J.*, 2025, **31**, e202501806.

45 G. Merino, M. Solà, I. Fernández, C. Foroutan-Nejad, P. Lazzeretti, G. Frenking, H. L. Anderson, D. Sundholm, F. P. Cossío, M. A. Petrukhina, J. Wu, J. I. Wu and A. Restrepo, Aromaticity: Quo Vadis, *Chem. Sci.*, 2023, **14**, 5569–5576.

46 J. Poater, S. Escayola, A. Poater, F. Teixidor, H. Ottosson, C. Viñas and M. Solà, Single-Not Double-3D-Aromaticity in an Oxidized Closo Icosahedral Dodecaiodo-Dodecaborate Cluster, *J. Am. Chem. Soc.*, 2023, **145**, 22527–22538.

47 M. Solà, Forty years of Clar's aromatic π-sextet rule, *Front. Chem.*, 2013, **1**, 22.

48 M. Solà, Why Aromaticity Is a Suspicious Concept? Why?, *Front. Chem.*, 2017, **5**, 22.

49 M. Solà, Aromaticity rules, *Nat. Chem.*, 2022, **14**, 585–590.

50 P. v. R. Schleyer, Introduction: Aromaticity, *Chem. Rev.*, 2001, **101**, 1115–1117.

51 R. F. W. Bader, Atoms in Molecules, *Acc. Chem. Res.*, 1985, **18**, 9–15.

52 F. Feixas, E. Matito, J. Poater and M. Solà, On the performance of some aromaticity indices: A critical assessment using a test set, *J. Comput. Chem.*, 2008, **29**, 1543–1554.

53 J. Poater, M. Solà, C. Viñas and F. Teixidor, A Simple Link between Hydrocarbon and Borohydride Chemistries, *Chem. – Eur. J.*, 2013, **19**, 4169–4175.

54 J. Poater, M. Solà, C. Viñas and F. Teixidor, π Aromaticity and Three-Dimensional Aromaticity: Two sides of the Same Coin?, *Angew. Chem., Int. Ed.*, 2014, **53**, 12191–12195.

55 J. Poater, M. Solà, C. Viñas and F. Teixidor, Hückel's Rule of Aromaticity Categorizes Aromatic closo Boron Hydride Clusters, *Chem. – Eur. J.*, 2016, **22**, 7437–7443.

56 G. te Velde, F. M. Bickelhaupt, E. J. Baerends, C. Fonseca Guerra, S. J. A. van Gisbergen, J. G. Snijders and T. Ziegler, Chemistry with ADF, *J. Comput. Chem.*, 2001, **22**, 931–967.

57 F. M. Bickelhaupt and E. J. Baerends, in *Reviews in Computational Chemistry*, ed. K. B. Lipkowitz and D. B. Boyd, Wiley-VCH, New York, 2000, vol. 15, pp. 1–86.

58 P. Vermeeren, T. A. Hamlin and F. M. Bickelhaupt, Chemical reactivity from an activation strain perspective, *Chem. Commun.*, 2021, **57**, 5880–5896.

59 P. Vermeeren, S. C. C. van der Lubbe, C. Fonseca Guerra, F. M. Bickelhaupt and T. A. Hamlin, Understanding chemical reactivity using the activation strain model, *Nat. Protoc.*, 2020, **15**, 649–667.

60 Z. F. Chen, C. S. Wannere, C. Corminboeuf, R. Puchta and P. V. Schleyer, Nucleus-independent chemical shifts (NICS) as an aromaticity criterion, *Chem. Rev.*, 2005, **105**, 3842–3888.

61 J. Poater, C. Viñas, M. Solà and F. Teixidor, Aromaticity and Extrusion of Benzenoids Linked to [o-COSAN]-. Clar has the Answer, *Angew. Chem., Int. Ed.*, 2022, **61**, e202200672.

62 K. Wolinski, J. F. Hinton and P. Pulay, Efficient Implementation of the Gauge-Independent Atomic Orbital Method for NMR Chemical-Shift Calculations, *J. Am. Chem. Soc.*, 1990, **112**, 8251–8260.

63 P. Bultinck, R. Ponec and S. Van Damme, Multicenter bond indices as a new measure of aromaticity in polycyclic aromatic hydrocarbons, *J. Phys. Org. Chem.*, 2005, **18**, 706–718.

64 F. Feixas, E. Matito, J. Poater and M. Solà, Quantifying aromaticity with electron delocalisation measures, *Chem. Soc. Rev.*, 2015, **44**, 6434–6451.

65 E. Matito, M. Duran and M. Solà, The aromatic fluctuation index (FLU): A new aromaticity index based on electron delocalization, *J. Chem. Phys.*, 2005, **122**, 014109.

66 E. Matito, ESI-3D: Electron Sharing Indices Program for 3D Molecular Space Partitioning, 2006.

67 E. Matito, M. Solà, P. Salvador and M. Duran, Electron sharing indexes at the correlated level. Application to aromaticity calculations, *Faraday Discuss.*, 2007, **135**, 325–345.

68 G. Monaco, F. F. Summa and R. Zanasi, Program Package for the Calculation of Origin-Independent Electron Current Density and Derived Magnetic Properties in Molecular Systems, *J. Chem. Inf. Model.*, 2021, **61**, 270–283.

69 G. Monaco, F. F. Summa and R. Zanasi, Atomic size adjusted calculation of the magnetically induced current density, *Chem. Phys. Lett.*, 2020, **745**, 137281.

70 R. J. F. Berger, G. Monaco and R. Zanasi, On the topology of total and diamagnetic induced electronic currents in molecules, *J. Chem. Phys.*, 2020, **152**, 194101.

71 A. D. Becke, Density-Functional Thermochemistry .3. The Role of Exact Exchange, *J. Chem. Phys.*, 1993, **98**, 5648–5652.

72 C. T. Lee, W. T. Yang and R. G. Parr, Development of the Colle-Salvetti Correlation-Energy Formula into a Functional of the Electron-Density, *Phys. Rev. B: Condens. Matter Mater. Phys.*, 1988, **37**, 785–789.

73 P. J. Stephens, F. J. Devlin, C. F. Chabalowski and M. J. Frisch, Ab-Initio Calculation of Vibrational Absorption and Circular-Dichroism Spectra Using Density-Functional Force-Fields, *J. Phys. Chem.*, 1994, **98**, 11623–11627.

74 G. Monaco, F. F. Summa, R. Zanasi and P. Lazzeretti, Electronic Current Density Induced by Uniform Magnetic Fields in Clarenes, *Chem. – Eur. J.*, 2024, **30**, e202401167.